Extension of the Hamaneh-Taylor model using the macroscopic polarization for the description of chiral smectic liquid crystals

H. Dhaouadi,* N. Bitri,† S. Essid, T. Soltani, and A. Gharbi
Laboratoire de Physique de la Matière Molle Faculté des Sciences de Tunis, 2092 El Manar Tunis, Tunisia

J. P. Marcerou‡
Centre de Recherches Paul Pascal, 115 Av. Albert-Schweitzer, 33600 Pessac, France

(Received 4 June 2009; published 28 September 2009)

Chiral smectic liquid crystals exhibit a series of phases, including ferroelectric, antiferroelectric, and ferrielectric commensurate structures as well as an incommensurate Sm-C^*_α phase. We carried out an extension of the phenomenological model recently presented by Hamaneh and Taylor based on the distorted-clock model. The salient feature of this model is that it links the appearance of phases to a spontaneous microscopic twist: i.e., an increment α of the azimuthal angle from layer to layer. The balance between this twist and an orientational order parameter J gives the effective phase. We introduce a second orientational order parameter I, which physical meaning comes from the macroscopic polarization; the effect of an applied electric is also studied. We derive phase diagrams and correlate them to our experimental results under field showing the sequence of phases versus temperature and electric field in some compounds.

DOI: 10.1103/PhysRevE.80.031712 PACS number(s): 61.30.Cz

I. INTRODUCTION

Chiral smectics are allowed to become ferroelectric and present a helical precession of the optical axes around the layer normal when a tilt of the molecules appears in the layers [1]. In the order of decreasing temperature and increasing tilt angle θ, one can observe a subset of the following full sequence [2–5]: the smectic-A (Sm-A) without tilt angle ($\theta=0$), the smectic-C^*_α (Sm-C^*_α) with a tilt angle θ, and an azimuthal angle Φ precessing with a short incommensurate period along the layer normal; the smectic-C^*(Sm-C^*) with Φ precessing with a long period and a helicity sign depending on chirality, it is locally ferroelectric ($P_S \neq 0$); the smectic-C^* Ferri2 (Sm-C^*_{Fi2}), where Φ is periodic over four layers and has a nonregular increment ($\Delta\Phi \neq 2\pi/4$) within the unit cell, the whole structure shows a long pitch helix with the same sign as the Sm-C^*, it has no macroscopic polarization ($P_S=0$); the smectic-C^* Ferri1 (Sm-C^*_{Fi1}), where Φ has a nonregular increment ($\Delta\Phi \neq 2\pi/3$) periodic over three layers, a long pitch helix with the opposite sign as in SmC^*, it is truly ferrielectric ($P_S \neq 0$); the smectic-C^*_A(Sm-C^*_A) with Φ periodic over two layers, a regular increment ($\Delta\Phi=\pi$), a long pitch helix with the opposite sign to Sm-C^*, it is referred to as antiferroelectric ($P_S=0$) or anticlinic. Some of these phases may be missing when varying the chemical formula (tail length) [6] but the order of appearance is conserved. Two of them present a macroscopic polarization; four of them a long pitch helical precession with a sign change in the middle of the sequence [7–9]. Although most of these phases present a biaxiality of the unit cell, the global structure is uniaxial because of the helical precession around the layer normal and an optical activity that can be huge results from the rotation of the biaxial structure [10]. Other nomenclatures are also adopted: Sm-$C^*_{Fi1} \rightarrow$ Sm-C^*_γ and Sm-$C^*_{Fi2} \rightarrow$ AF [2,11]. To characterize the different phases, several experimental methods can be used: optical observations, calorimetric measurements, and resonant x-ray scattering [3,4]. Other subphases have been proposed [12–14] but are linked to assumptions which are not accepted unanimously.

Let us briefly mention some theoretical models, which have been proposed to describe the structures and behavior of chiral smectic liquid crystals. The devil's staircase model, also called Ising model because only one direction is allowed for the azimuth, was proposed soon after the discovery of the tilted smectic subphases by Chandani *et al.* [2,12,15]. It is based on the assumption that the competition between the synclinic sequence (where one layer and the following one have the same azimuth) and the anticlinic one (opposite azimuths) is at the origin of subphases, which present a periodic succession of such sequences. An infinite number of phases with various ratios of synclinic versus anticlinic sequences are predicted making the so-called devil's staircase [12]. One can define the q_T index as the fraction $S/(S+A)$ of synclinic ordering versus the total number. Unfortunately, the same index applies to phases with different symmetries so it is simply irrelevant. This model is still supported [13], although it has been ruled out by the results of x-ray resonant scattering experiments [16].

The nearest-neighbors models are based on the definition of a quantity often called $\xi_{\alpha z}$, which measures the tilt inside a layer by the coordinates of the c director [17],

$$\begin{pmatrix} \xi_{xz} \\ \xi_{yz} \end{pmatrix} = \begin{pmatrix} \sin\theta\cos\Phi \\ \sin\theta\sin\Phi \end{pmatrix}. \quad (1)$$

When $\xi_{\alpha z}$ is considered as the macroscopic order parameter, it can be chosen to describe the Sm-A to Sm-C phase

*hassen.dhaouadi@ipeit.rnu.tn
†Also at Centre de Recherches Paul Pascal, 115, Av. Albert-Schweitzer, 33600 Pessac, France.
‡marcerou@crpp-bordeaux.cnrs.fr; http://www.crpp-bordeaux.cnrs.fr

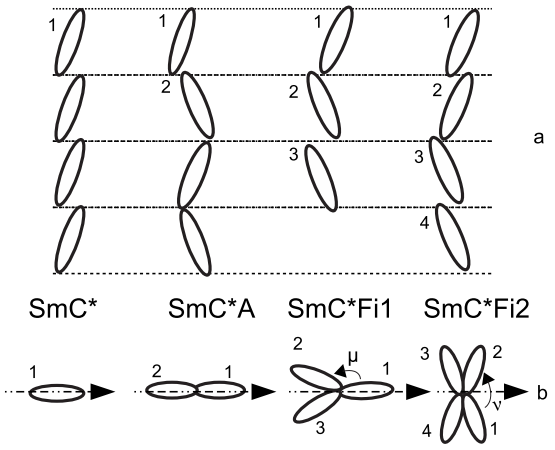

FIG. 1. Schematic description of the different phases in the distorted-clock model. (a) Side view (same tilt angle θ) period p of 1 to 4 layers; (b) top view (periodic azimuth such that $\Phi_{l+p}=\Phi_l+2\pi$). $\Delta\Phi=\nu$ or $\Delta\Phi=\pi-\nu$ in the Sm-C^*_{Fi2} and $\Delta\Phi=\mu$ or $\Delta\Phi=2(\pi-\mu)$ in the Sm-C^*_{Fi1}. Arrows indicate the direction Φ_0 taken as the origin of azimuthal angles. Any gap or overlap between molecules is due to the hand made drawing and has no physical meaning.

transition [18,19], as its modulus is nearly proportional to the tilt angle θ. If one considers it at the layer level, defining a different $\xi^j_{\alpha z}$ for each layer j, it can be used to build up a local free energy taking into account the interactions between layers. Theories have been proposed, which deal with these interactions by means of nearest-neighbors couplings $\xi^j\xi^{j+1}$ or next-nearest-neighbors $\xi^j\xi^{j+2}$. The form of the free energy is discrete as one has to sum up the interaction terms over all layers in the integration domain. One can find theories by Sun *et al.* [20], Roy and Madhusudana [21,22], and Vaupotic and Cepic [23]. In all cases, a suitable combination of coupling terms could lead to phase diagrams compatible with existing phases. Lorman introduced linear combinations of this parameter $\xi_{\alpha z}$ over up to four layers [24] and his treatment led to the prediction of the well-known tilted subphases, except for the Sm-C^*_α phase.

From an experimentalist's point of view, these models are of little usefulness and it is better to stay in the frame of the distorted-clock model as it gives the best description of the currently encountered phases.

A. Distorted-clock model

This is a purely experimental model describing the observations without *ab initio* theory also called the *XY* model because all the azimuthal directions in the layer plane are allowed. It has been derived by modeling the orientation of the molecules in the layers and then fitting the resonant scattering experiments with success. With consecutive iterations of the initial regular model [4,16], the authors have introduced some asymmetries in the azimuthal angle distribution as it is reported in Fig. 1. The model is still in evolution concerning the Sm-C^*_α phase [5,25], but it is coherent and is at the base of the calculations reported here.

B. Hamaneh-Taylor model

It is only recently that a new phenomenological way to describe the chiral smectic phases was proposed [26,27] that we call afterward as the Hamaneh-Taylor (H&T) model. It is based on the balance between a short-range twisting term trying to impose an increment α of the azimuthal angle between adjacent layers and a long-range term linked to the anisotropy of curvature energy in the layer planes. They derived an order parameter $J=\langle\cos 2\Phi_l\rangle$, where the average is taken on the azimuthal angles inside the unit cell. It is nonnull in the phases enumerated above and associated to an energy ηJ^2, where η is a coefficient that describes the strength of the long-range interactions. The short-order term reads as $\langle\cos(\Delta\Phi-\alpha)\rangle$ with $\Delta\Phi=\Phi_l-\Phi_{l-1}$, the elastic term is ηJ^2, and the free energy of the sample is

$$\frac{F}{F_0}=\langle\cos(\Delta\Phi-\alpha)\rangle+\eta J^2. \tag{2}$$

The order of magnitude of F_0 is the electrostatic energy $(-P_S\cdot E_c)$ necessary to drive at the field E_c, the phase transition to a ferroelectric phase with a polarization P_S [26,27], while η is on the order of unity.

This leads to a phase diagram in the (η,α) plane, showing the sequences of subphases, which can be observed in a given liquid crystal. This model presents some limitations. First, it introduces a phase with six layers, which was never observed experimentally. Second, the extent of the three layers phase is very small.

After this review, we introduce in the next sections a new orientational order parameter I that will describe the contribution of the macroscopic polarization P_S to the ordering. We present then the phases diagrams obtained from a numerical calculation. Eventually, we compare the theoretical results with our experimental data obtained on several compounds

II. ORIENTATIONAL ORDER PARAMETER

In H&T model, it is shown clearly that the average $J=\langle\cos 2\Phi_l\rangle$ is nonzero in all the phases described by the distorted-clock model, by analogy we state that another average $I=\langle\cos\Phi_l\rangle$ is also non-null in the phases, such as Sm-C^* and Sm-C^*_{Fi1}, which possess a macroscopic polarization. The origin Φ_0 is such that the averages over sine functions are zero [26,27]; it will be the azimuth Φ_1 of the first layer, except in the Sm-C^*_{Fi2} phase, where it is equal to $\Phi_1+\nu/2$. We get the following table, where μ and ν stand for the characteristic angles of asymmetry in the Ferri phases.

A. Introduction of an I^2 term in the free energy

The symmetry argument of Meyer [1] stating that there exists a polarization P as soon as the layer normal $\vec{N}$ and the director $\vec{n}$ make an angle θ can be translated by introducing in the free energy the mixed product of $\vec{P}$, $\vec{N}$, and $\vec{n}$. Taking into account Table I, the angle between $\vec{N}$ and $\vec{n}$ reads as $I\theta$, so with the addition of the self-energy of the polarization, one gets

$$\Delta F_P=\frac{P^2}{2\varepsilon_0\chi}-CPI\theta, \tag{3}$$

by minimizing over P, one finds

TABLE I. Order parameters I and J and origin of angles in the different phases.

	$I=\langle\cos\Phi_l\rangle$	$J=\langle\cos 2\Phi_l\rangle$	origin Φ_0
Sm-C^*_α	0	0	X
Sm-C^*	1	1	Φ_1
Sm-C^*_A	0	1	Φ_1
Sm-C^*_{Fi1}	$[1+2\cos\mu]/3$	$[1+2\cos 2\mu]/3$	Φ_1
Sm-C^*_{Fi2}	0	$-\cos\upsilon$	$\Phi_1+\upsilon/2$

$$P_S=\varepsilon_0\chi CI\theta,$$

$$\Delta\tilde{F}_P=-\frac{P_S^2}{2\varepsilon_0\chi}=-\frac{\varepsilon_0\chi C^2\theta^2}{2}I^2. \tag{4}$$

We have thus demonstrated that the term due to the macroscopic polarization P_S, present only when I is nonzero, can be written $\tilde{\gamma}\theta^2I^2$ and we can add it to H&T free energy after a little bit of algebra on the orientational order parameter.

B. Relationship between I^2 and J^2 terms

Let us start from the de Gennes orientational order parameter in the Sm-A phase; in what follows one considers the z axis to be perpendicular to the smectic layers,

$$Q^0_{ij}=n_in_j-\frac{1}{3}\delta_{ij}=\begin{pmatrix}-1/3 & 0 & 0\\ 0 & -1/3 & 0\\ 0 & 0 & +2/3\end{pmatrix}. \tag{5}$$

One can build up an orientational order parameter Q_{ij} for all the tilted phases of the distorted-clock model by first computing for each layer, in an axis frame where z is the layer normal, the expression of Q^0_{ij} after a tilt of the director $\vec{n}$ by an angle θ. This rotation is made around an axis inside the layer such that Φ is the angle between the c director (projection of the director $\vec{n}$ in the layer plane) and the x axis,

$$Q^{\theta\Phi}_{ij}=\left(1-\frac{3}{2}\sin^2\theta\right)\begin{pmatrix}-1/3 & 0 & 0\\ 0 & -1/3 & 0\\ 0 & 0 & +2/3\end{pmatrix}+\frac{1}{2}\sin^2\theta\begin{pmatrix}\cos 2\Phi & \sin 2\Phi & 0\\ \sin 2\Phi & -\cos 2\Phi & 0\\ 0 & 0 & 0\end{pmatrix}-\sin\theta\cos\theta\begin{pmatrix}0 & 0 & \cos\Phi\\ 0 & 0 & \sin\Phi\\ \cos\Phi & \sin\Phi & 0\end{pmatrix}. \tag{6}$$

Finally, Q_{ij} is computed by averaging over the unit cell of each phase. For the Sm-C^*_α, the average over Φ is null for the second and the third matrices and there remains

$$Q^{\alpha}_{ij}=\left(1-\frac{3}{2}\sin^2\theta\right)\begin{pmatrix}-1/3 & 0 & 0\\ 0 & -1/3 & 0\\ 0 & 0 & +2/3\end{pmatrix}. \tag{7}$$

For all other phases, one can write a general formula for Q_{ij}, which is a function of Φ_0 defined in Table I, as the angle between the origin of azimuthal angles in the unit cell and the x axis. The resulting order parameter Q_{ij} is unique; it is only its expression in a given frame, which depends on Φ_0. One readily finds that the order parameters $J=\langle\cos 2\Phi_l\rangle$ and $I=\langle\cos\Phi_l\rangle$ can be factorized in the last two matrices. For example, in the Sm-C^*_{Fi1} phase, where $\Phi_1=\Phi_0,\Phi_2=\Phi_0+\mu,\Phi_3=\Phi_0-\mu$, the averages in the unit cell give $(\cos\Phi_1+\cos\Phi_2+\cos\Phi_3)=3I\cos\Phi_0$, $(\cos 2\Phi_1+\cos 2\Phi_2+\cos 2\Phi_3)=3J\cos 2\Phi_0$, $(\sin\Phi_1+\sin\Phi_2+\sin\Phi_3)=3I\sin\Phi_0$, $(\sin 2\Phi_1+\sin 2\Phi_2+\sin 2\Phi_3)=3J\sin 2\Phi_0$, and so on for all the phases,

$$Q_{ij}=\left(1-\frac{3}{2}\sin^2\theta\right)\begin{pmatrix}-1/3 & 0 & 0\\ 0 & -1/3 & 0\\ 0 & 0 & +2/3\end{pmatrix}+\frac{J}{2}\sin^2\theta\begin{pmatrix}\cos 2\Phi_0 & \sin 2\Phi_0 & 0\\ \sin 2\Phi_0 & -\cos 2\Phi_0 & 0\\ 0 & 0 & 0\end{pmatrix}-I\sin\theta\cos\theta\begin{pmatrix}0 & 0 & \cos\Phi_0\\ 0 & 0 & \sin\Phi_0\\ \cos\Phi_0 & \sin\Phi_0 & 0\end{pmatrix}. \tag{8}$$

It is straightforward to remark that the only parameters that should be retained for building the free energy are the factorized matrix coefficients $J\sin^2\theta\sim\theta^2J$ and $I\sin\theta\cos\theta\sim\theta I$. So the H&T term should read as $\tilde{\eta}\theta^4J^2$ and the polarization term as demonstrated above $\tilde{\gamma}\theta^2I^2$. We took advantage of this by considering that we could write the modified H&T free energy under the form,

$$\frac{F}{F_0}=\langle\cos(\Delta\Phi-\alpha)\rangle+\tilde{\eta}\theta^4J^2+\tilde{\gamma}\theta^2I^2=\langle\cos(\Delta\Phi-\alpha)\rangle+\eta J^2+\gamma\sqrt{\eta}I^2. \tag{9}$$

We then assume that the temperature dependence of the η coefficient is due to $\theta^4\sim(T_c-T)^2$, where T_c is the temperature of appearance of the tilt angle and that the coefficient γ depends only on the compound and not on the temperature. We eventually build phase diagrams in the (η,α) plane, each one for a different value of γ taking it to be on the order of unity, from 0 to 1 (see, e.g., Fig. 2). These results show that the Sm-C^* and Sm-C^*_{Fi1} domains grow with γ, i.e., with the permanent polarization, let us consider now what happens in the presence of an external electric, which is known to induce phase transitions to polar phases [28].

C. Effect of electric field in the layer plane

An electric field applied to the sample always creates a small dielectric polarization proportional to it, which is the same in all studied phases to first approximation. But when there is already a spontaneous polarization P_S, it will displace the energy by a term, which reads roughly $-P_S\cdot E$. The free energy can be written by slightly modifying Eq. (3),

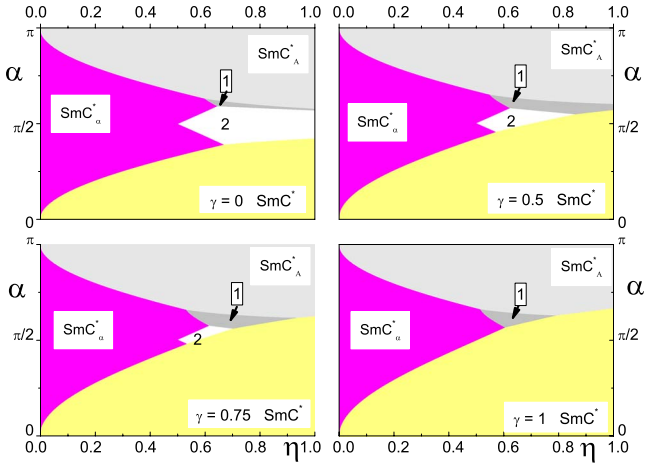

FIG. 2. (Color online) Ground-state diagram for γ=0, 0.5, 0.75, and 1. The symbols 1 and 2 stand for Ferri1 and Ferri2.

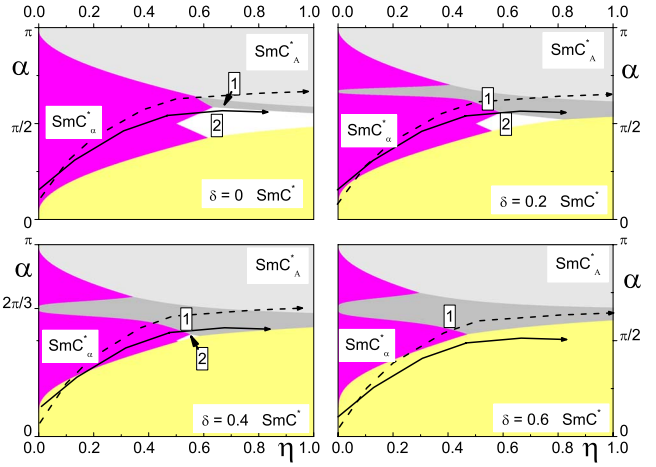

FIG. 3. (Color online) Diagrams obtained with applied field for γ=0.2 and δ=0, 0.2, 0.4, and 0.6. The black plain curve corresponds to an estimate of the path $\eta(\alpha)$ followed by C10F3 and the dotted line to $\eta(\alpha)$ for C7F2.

$$\Delta F_E = \frac{P^2}{2\varepsilon_0\chi} - CPI\theta - P\cdot E - \frac{\varepsilon_\perp E^2}{2}, \tag{10}$$

by minimizing over P, one finds

$$\tilde{P} = \varepsilon_0\chi(C\theta I + E) = P_S + \varepsilon_0\chi E,$$

$$\Delta\tilde{F}_E = -\frac{P_S^2}{2\varepsilon_0\chi} - P_S\cdot E - \frac{\tilde{\varepsilon}_\perp E^2}{2}. \tag{11}$$

For a given value of the electric field, the third term $-\tilde{\varepsilon}_\perp E^2/2$ is the same for all the phases and does not depend on the orientational order parameters I and J so we simply forget about it. The first two terms have the same order of magnitude $F_0 \sim -P_S\cdot E_c$ and are, respectively, quadratic and linear versus θ, so by taking η as the main parameter, we can write down

$$\frac{F}{F_0} = \langle\cos(\Delta\Phi - \alpha)\rangle + \eta J^2 + \gamma\sqrt{\eta}I^2 + \delta\sqrt[4]{\eta}I. \tag{12}$$

We use this expression to compute the phase diagrams in the (η,α) plane, each one for a different value of γ and δ (see, e.g., Fig. 3).

III. NUMERICAL STUDY AND PHASE DIAGRAMS

In the different phases of the distorted-clock model represented on the Fig. 1, we establish at first the expression of the free energy for a given (η,α) by computing the order parameters I and J as well as the quantity $\langle\cos(\Delta\Phi-\alpha)\rangle$ for each structure. The H&T model predicts the existence of a phase with six layers. We are going to disregard this phase, on one hand, by the fact that it was never observed; on the other hand, because it disappears of the diagram once the term due to the polarization P_S is added. Other structures not observed experimentally have been briefly tested like a four layer asymmetric phase, which has a less favorable energy than the Ferri2 phase. Let us point out that as F_0 is negative, we look for an absolute maximum of F/F_0 to get the best phase.

(i) In the Sm-C^*_α phase, the short-order term reduces to 1, while the additional terms vanish. J=0 and I=0; thus the free energy is $F=F_0$

(ii) In the Sm-C^* phase, J=1 and I=1; thus

$$\frac{F}{F_0} = \eta + \cos\alpha + \gamma\sqrt{\eta} + \delta\sqrt[4]{\eta}. \tag{13}$$

(iii) In the Sm-C^*_A phase, J=1 and I=0; thus

$$\frac{F}{F_0} = \eta - \cos\alpha. \tag{14}$$

(iv) In the Sm-C^*_{Fi2} phase $J=-\cos\upsilon$, I=0, and by minimizing F over υ, we find for $\eta>0.5$ that the preferred angle is such that $\sin\tilde{\upsilon}=\sin\alpha/2\eta$ and the free energy reads as

$$\frac{F}{F_0} = \eta + \frac{\sin^2\alpha}{4\eta}. \tag{15}$$

(v) In the Sm-C^*_{Fi1} phase, $J=(1+2\cos 2\mu)/3$, $I=(1+2\cos\mu)/3$, so all the terms of Eq. (12) must be explicit,

$$\langle\cos(\Delta\Phi-\alpha)\rangle = [2\cos(\mu-\alpha)+\cos(2\mu+\alpha)]/3,$$

$$\eta J^2 = \eta(4\cos^2\mu - 1)^2/9,$$

$$\gamma\sqrt{\eta}I^2 = \gamma\sqrt{\eta}(2\cos\mu + 1)^2/9,$$

$$\delta\sqrt[4]{\eta}I = \delta\sqrt[4]{\eta}|2\cos\mu + 1|/3. \tag{16}$$

The maximization of the energy has to be made numerically giving the preferred value of μ and F/F_0.

A. Computation of phase diagrams

Let us first discuss the physical meaning of these diagrams. On the x axis, one reports the values of the parameter η that we take in mean-field approximation as being the

fourth power of the tilt angle θ; thus the second power of the distance in temperature from the Sm-A phase, i.e., the tilt angle appears at the Sm-A to Sm-C phase transition and follows a $\sqrt{T_c - T}$ law. So the x axis represents decreasing temperatures from the Sm-A at left to the right. The y axis shows the scale of variation in the *ad hoc* angle α from 0 to π. This parameter makes the richness of the H&T model; it means physically that due to the chirality the director wants to be twisted from layer to layer by the angle α and it is the balance between this tendency and a more uniform azimuthal angle distribution measured by the I and J order parameters that gives rise to the effective structures. It is remarkable that with so few parameters, one can get all the structures determined experimentally before the theory was developed by H&T. One is not as usual trying to fit the experiment to a theory imposed *ab initio*. What we introduce in this paper are new terms linked to the polar nature of two phases in the tilted chiral smectics nomenclature: the Sm-C^* and the Sm-C^*_{Fi1}. We express these terms as functions of the x-axis parameter; one measuring the spontaneous polarization and the other its coupling with external field. Our aim is to show that the domain filled in by these two phases will be extended in the diagram.

We first present in Fig. 2 some diagrams obtained for different values of γ that correspond to the ground states without applied field. As γ increases, one notices an expansion of the domains corresponding to the Sm-C^* and Sm-C^*_{Fi1} phases, which are the only ones with a spontaneous polarization. It is to be noticed that for $\gamma=1$, the domain corresponding to Sm-C^*_{Fi2} has completely disappeared.

The diagram obtained with $\gamma=0.2$ is chosen to illustrate qualitatively (Fig. 3) the sequences of phases, which appear for the two compounds we have studied experimentally in our group: the C10F3 and the C7F2 [6,28–30].

With the applied field, i.e., the parameter δ one notices also an expansion of the Sm-C^* and Sm-C^*_{Fi1} domains. Furthermore, it appears a band corresponding to Sm-C^*_{Fi1} in full center of the alpha domain; this band widens gradually as δ increases.

B. Comparison with experiment

In Fig. 3 are represented estimated paths followed on decreasing the temperature by two compounds studied experimentally in our group: the C7F2 (dotted curve) and C10F3 (plain). The paths are unchanged in the different panels of the figure as they depend only on the temperature; the nature of the phase encountered at a given point changes as the Sm-C^*_{Fi1} and Sm-C^* domains grow.

The C7F2 compound shows the following ground phase sequence: Sm$A \rightarrow$ Sm-$C^*_\alpha \rightarrow$ Sm-C^*_A. The corresponding path (dotted line in Fig. 3) has to include the (Sm-C^*_α) $-$(Sm-C^*_{Fi1})$-$(Sm-C^*_A) triple point (below arrow as in Fig. 4) as a very weak field reveals the Sm-C^*_{Fi1} phase. The increase in the electric field enlarges the Sm-C^* and Sm-C^*_{Fi1} domains. At a certain point, the path crosses the Sm-C^* domain then the Sm-C^*_α and the Sm-C^*_{Fi1} finishing in the Sm-C^*_A (b and c in Fig. 4). For a large enough field, the SmC^* domain will cover almost all the length of the path (arrow d).

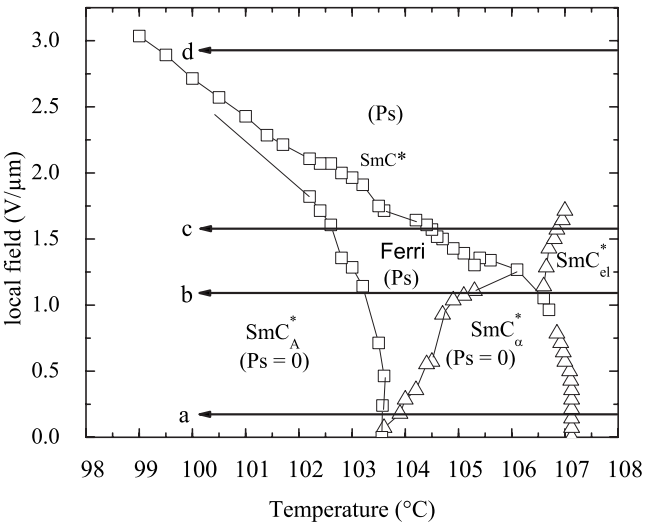

FIG. 4. (E,T) phase diagram of the compound C7F2. The constant field paths a to d correspond to increasing values of the parameter δ.

The C10F3 compound presents at zero field the following phase sequence: Sm-$A \rightarrow$ Sm-$C^*_\alpha \rightarrow$ Sm-C^*_{Fi2}. For weak electric field (arrow a′ in Fig. 5), the sequence remains almost the same. For a higher electric field (arrow b′), the curve corresponding to the C10F3 begins in the Sm-C^* domain then passes in the Sm-C^*_α before the Sm-C^*_{Fi1} grows bigger at the expense of the Sm-C^*_{Fi2} domain. One then encounters successively two triple points: the (Sm-C^*_α)$-$(Sm-C^*_{Fi1}) $-$(Sm-C^*_{Fi2}) and the (Sm-C^*)$-$(Sm-C^*_α)$-$(Sm-C^*_{Fi1}). For a strong electric field, the Sm-C^* phase is dominant (arrow c′).

C. Discussion

Another comparison to experiment can be made with the published values of the distortion angles μ and υ. Cady *et al.*

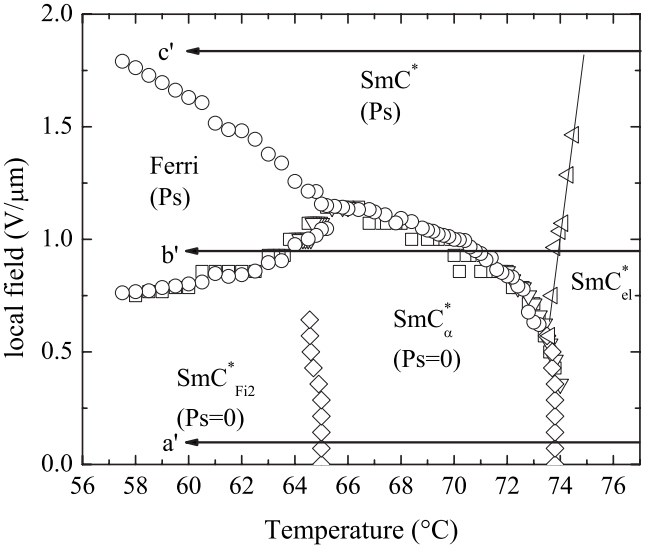

FIG. 5. (E,T) phase diagram of the compound C10F3. The constant field paths a′ to c′ correspond to increasing values of the parameter δ.

[3] found for the Sm-C^*_{Fi2} structure a value of υ of about 164°, Roberts *et al.* [31] measured the angular distortion of the Sm-C^*_{Fi2} and Sm-C^*_{Fi1} structures in mixtures at two temperatures; they found a value of υ of about 166° and that of μ of about 152°–160° with no discernable dependence on temperature. Starting from our equations, we made the calculation of υ and μ for different points from the two curves of Fig. 3. We found values of μ varying from 156° to 161° for both compounds (under field), which is comparable to that reported by Cady *et al.* and Roberts *et al.* [3,31]. On the other hand, the values we computed for the υ angle, about 142°, are slightly lower than the measured values [31,32] but still far from the regular clock model (υ=90°).

We have shown that taking into account the macroscopic polarization in H&T theory, one is led to an expansion of the Sm-C^* and Sm-C^*_{Fi1} existence domains, which is correlated with the (E-T) phase diagrams we have obtained experimentally.

As noticed by H&T, the translation of the theory in a quantitative way requires the knowledge of the physical path $\alpha(\eta)$ or separately $\alpha(T)$ and $\eta(T)$. What we add is the requirement for the new γ and δ parameters, which can be derived from the measurement of P_S and E [see, e.g., Eq. (11)]. The parameter η should be considered to be zero at the temperature T_c, where the tilt angle appears and to follow a $(T_c-T)^2$ law below. In the H&T frame, it gets remarkable values at the phase boundaries such as $\eta=1+\cos\alpha$ at the Sm-C^*_α to Sm-C^*_A phase transition. So the measurement of α in the Sm-C^*_α phase is required.

Several experimental methods have been reported to measure the parameter α; let us quote the resonant x-rays diffraction, which allows to measure a periodicity ranging usually from eight to three layers in Sm-C^*_α with a decrease (i.e., an increase in α) when cooling down the sample [5,16,25,33]. However, there are a few exceptions where the periodicity varies from about ten to 50 layers (α is decreasing) when lowering the temperature in the assumed Sm-C^*_α range [4,33]. This is not obviously an experiment accessible to everyone. Differential optical reflectivity has been also used to acquire the temperature variation in the helical pitch in the Sm-C^*_α phase and has also shown an increase in α when cooling down [34]. Another method used by Isaert and coworkers [35] consists in measuring the spacing of the Friedel fringes, which appear in the reflected light texture on the free surface of drops; this simple method could allow a fast measurement of α. Finally, another candidate is the gyrotropic method given by Ortega *et al.* [36] who, by a measurement of the ellipticity of eigenmodes, claimed to get the pitch and thus the angle α.

IV. CONCLUSION

In this paper, we report a successful method for the description of chiral smectic liquid crystals based on the Hamaneh-Taylor model. The introduction of the polarization and the electric field contributions give results that sound in good agreement with experiment and allow explaining the appearance under field of an intermediate ferrielectric phase. The measurement of the parameter α and of the polarization P_S should allow to trace the paths followed by a given compound in the (η,α) plane. In the future, we plan to introduce the helicity and its sign evolution in the phase sequence.

ACKNOWLEDGMENTS

We wish to acknowledge the support of CMCU Grant No. 06/G 1311 and CNRS/DGRSRT Grant No. 18476.

[1] R. B. Meyer, L. Liebert, L. Strzelecki, and P. Keller, J. Phys. (Paris) Lett. **36**, L69 (1975).
[2] A. D. L. Chandani, E. Gorecka, Y. Ouchi, H. Takezoe, and A. Fukuda, Jpn. J. Appl. Phys. **28**, L1265 (1989).
[3] A. Cady *et al.*, Phys. Rev. E **64**, 050702(R) (2001).
[4] L. S. Hirst *et al.*, Phys. Rev. E **65**, 041705 (2002).
[5] D. A. Olson, X. F. Han, A. Cady, and C. C. Huang, Phys. Rev. E **66**, 021702 (2002).
[6] S. Essid, M. Manai, A. Gharbi, J. P. Marcerou, H. T. Nguyen, and J. C. Rouillon, Liq. Cryst. **31**, 1185 (2004).
[7] Hl. de Vries, Acta Crystallogr., Sect. A: Cryst. Phys., Diffr., Theor. Gen. Crystallogr. **4**, 219 (1951).
[8] F. Beaubois, J. P. Marcerou, H. T. Nguyen, and J. C. Rouillon, Eur. Phys. J. A **3**, 273 (2000).
[9] N. Bitri, A. Gharbi, and J. P. Marcerou, Physica B **403**, 3921 (2008).
[10] F. Beaubois, J. P. Marcerou, H. T. Nguyen, and J. C. Rouillon, Liq. Cryst. **26**, 1351 (1999).
[11] J. Lee, A. D. L. Chandani, K. Itoh, Y. Ouchi, H. Takezoe, and A. Fukuda, Jpn. J. Appl. Phys. **29**, 1122 (1990).
[12] A. Fukuda, Y. Takanishi, T. Isozaki, K. Ishikawa, and H. Takezoe, J. Mater. Chem. **4**, 997 (1994).
[13] N. M. Shtykov, A. D. L. Chandani, A. V. Emelyanenko, A. Fukuda, and J. K. Vij, Phys. Rev. E **71**, 021711 (2005).
[14] H. F. Gleeson, L. Baylis, W. K. Robinson, J. T. Mills, J. W. Goodby, A. Seed, M. Hird, P. Styring, C. Rosenblatt, and S. Zhang, Liq. Cryst. **26**, 1415 (1999).
[15] T. Matsumoto, A. Fukuda, M. Johno, Y. Motoyama, T. Yui, S. S. Seomun, and M. Yamashita J. Mater. Chem. **9**, 2051 (1999).
[16] P. Mach, R. Pindak, A. M. Levelut, P. Barois, H. T. Nguyen, C. C. Huang, and L. Furenlid, Phys. Rev. Lett. **81**, 1015 (1998).
[17] P. G. de Gennes and J. Prost, *The Physics of Liquid Crystals*, 2nd ed. (Clarendon Press, Oxford, 1993).
[18] T. Carlsson, B. Zeks, A. Levstik, C. Filipic, I. Levstik, and R. Blinc, Phys. Rev. A **36**, 1484 (1987).
[19] H. Orihara and Y. Ishibashi, Jpn. J. Appl. Phys. **29**, L115 (1990).
[20] H. Sun, H. Orihara, and Y. Ishibashi, Jpn. J. Appl. Phys. **60**, 4175 (1991).
[21] A. Roy and N. Madhusudana, Europhys. Lett. **36**, 221 (1996).
[22] A. Roy and N. Madhusudana, Eur. Phys. J. E **1**, 319 (2000).
[23] N. Vaupotic and M. Cepic, Phys. Rev. E **71**, 041701 (2005).
[24] V. Lorman, Liq. Cryst. **20**, 267 (1996).
[25] Z. Q. Liu *et al.*, Phys. Rev. Lett. **99**, 077802 (2007).

[26] M. B. Hamaneh and P. L. Taylor, Phys. Rev. Lett. **93**, 167801 (2004).
[27] M. B. Hamaneh and P. L. Taylor, Phys. Rev. E **72**, 021706 (2005).
[28] J. P. Marcerou, H. T. Nguyen, N. Bitri, A. Gharbi, S. Essid, and T. Soltani, Eur. Phys. J. E **23**, 319 (2007).
[29] M. Manai, A. Gharbi, S. Essid, M. F. Achard, J. P. Marcerou, H. T. Nguyen, and J. C. Rouillon, Ferroelectrics **343**, 27 (2006).
[30] S. Essid, N. Bitri, H. Dhaouadi, A. Gharbi, and J. P. Marcerou, Liq. Cryst. **36**, 359 (2009).
[31] N. W. Roberts *et al.*, Europhys. Lett. **72**, 976 (2005).
[32] P. M. Johnson, D. A. Olson, S. Pankratz, H. T. Nguyen, J. Goodby, M. Hird, and C. C. Huang, Phys. Rev. Lett. **84**, 4870 (2000).
[33] A. Cady, D. A. Olson, X. F. Han, H. T. Nguyen, and C. C. Huang, Phys. Rev. E **65**, 030701(R) (2002).
[34] A. Cady, X. F. Han, D. A. Olson, H. Orihara, and C. C. Huang, Phys. Rev. Lett. **91**, 125502 (2003).
[35] V. Laux, N. Isaert, G. Joly, and H. T. Nguyen, Liq. Cryst. **26**, 361 (1999).
[36] J. Ortega, C. L. Folcia, J. Etxebarria, and M. B. Ros, Liq. Cryst. **30**, 109 (2003).